Clays and Clay Minerals, Vol. 53, No. 1, 71–91, 2005.

EUSTATIC AND TECTONIC/VOLCANIC CONTROL IN SEDIMENTARY BENTONITE FORMATION – A CASE STUDY OF MIOCENE BENTONITE DEPOSITS FROM THE PANNONIAN BASIN

ZOLTÁN PÜSPÖKI[1,*], MIKLÓS KOZÁK[1], PÉTER KOVÁCS-PÁLFFY[2], MARIA FÖLDVÁRI[2], RICHARD W. MCINTOSH[1] AND LÁSZLÓ VINCZE[1]

[1] Department of Mineralogy and Geology, University of Debrecen, Egyetem tér 1. Debrecen, H-4032, Hungary
[2] Geological Institute of Hungary, Stefánia út 14. Budapest, H-1142, Hungary

Abstract—Seven sedimentary bentonite deposits were investigated in the Miocene series of the Pannonian Basin. The following stratigraphic and genetic characteristics were significant: (1) all deposits were formed within a transgressive series of a given Miocene sequence; and (2) it is possible that the source material of the bentonites is rhyolitic, confirmed by radiometric data proving simultaneous rhyolite tuff volcanism.

A detailed investigation on three lithologically different bentonite horizons within the same transgressive series was made at Sajóbábony to determine the source material and to determine the causes of the differences. X-ray diffraction, differential thermal analysis and geochemical data of the different lithological types show that they all have rhyolitic source material, although in the case of the lowermost horizon the existence of reworked material from an underlying andesite tuff series is also presumed. The main difference is the degree of weathering. Considering the ratio between the amorphous phase and the montmorillonite, the amorphous volcanic glass can be regarded as the main source of the montmorillonite formation. The differences in the degree of alteration can be related to the changing characteristics of the tuff accumulation and the sedimentation. Transgression decreases the sedimentation rate allowing the optimal alteration of the amorphous phase. The increasing intensity of the tuff accumulation can also limit the bentonite formation because rapid deposition and burial present too little time for the optimal alteration of the amorphous phase.

Summarizing the results from the stratigraphic interpretation of the bentonite deposits and from the comparative analyses of the different bentonite horizons within the same transgressive systems tract, we can state that the relationship of the tectonic-related tuff accumulation and the eustasy-related sedimentation rate can affect both the possibility of bentonite formation in macro-scale and the degree of bentonitization in micro-scale.

Key Words—Bentonite, Miocene, Pannonian Basin, Rhyolite Tuff, Sequence Stratigraphy, Tectonics.

INTRODUCTION

During the past decade the Department of Mineralogy and Geology at the University of Debrecen has carried out geological mapping of the East Borsod Basin in North Hungary in the course of which a significant sedimentary bentonite deposit (in Central European terms) was discovered in the upper part (Sarmatian stage) of the Miocene series. Due to its potential economic importance a national research programme provided funding for further investigation of the bentonite deposit by deep drilling.

As a result of the stratigraphic and mineralogical analysis a genetic model was outlined for the formation of the bentonite deposit that emphasizes the role of accompanying eustatic and tectonic events. Moreover, considering different time scales, changes in the relationship between eustasy and tectonic-related volcanic events determined not only the occurrence of sedimentary bentonite deposits but even the quality of the sedimentary bentonite formed.

We suggest that these phenomena might be important not only from the bentonite exploration point of view but also in the course of modeling medial and short-term changes in eustatic curves. Therefore, to test the model, we examined the most important sedimentary bentonite deposits in the Pannonian Basin from the point of view of their source material and stratigraphic position. In this paper the results of data collection and experiences with the NE Hungarian deposit demonstrate the kind of eustatic, volcanic and tectonic events that lead to the formation of sedimentary bentonites and show how they can affect the facies type and the quality of the preserved bentonites.

First we give a brief outline of the structural background for the Miocene rhyolite tuff volcanic activity and the eustatic development of the Pannonian Basin. Then we demonstrate the stratigraphic position, mineralogical and geochemical characteristics and genetic interpretation of the economically important bentonite deposits referred to here as 'reference bento-

* E-mail address of corresponding author:
puspokiz@puma.unideb.hu
DOI: 10.1346/CCMN.2005.0530108

nite deposits' from the Pannonian Basin focusing on the similarities with the recently explored deposit. After this we will show some essential mineralogical and geochemical data of this deposit to prove the common genetic source and different lithological types and varying quality of the bentonite layers within the same deposit.

GEOLOGICAL BACKGROUND

Structural development and paleogeography of the Pannonian Basin in the Miocene

The Cretaceous-Paleogene tectonic development of the Pannonian basin is somewhat controversial. Some scientists account for facies differences as due to major strike-slip movements of the two micro-plates forming the basement of the present Pannonian Basin (Kovács, 1982). Others explain the facies differences by rotation and strike-slip movement (Balla, 1986; Schmidt *et al.*, 1991). There are also suggestions for very limited strike-slip movements and considering the major faults as reverse faults displaying an imbricated structure that is the result of rapid shortening and rotation (Kozák *et al.*, 2001).

However, about the structural development in the Miocene, there is greater concensus that it involved the extension of the inner Carpathians simultaneously with the emergence and deformation of the outer Carpathians (Horváth and Royden, 1981; Horváth, 1993). According to Tari *et al.* (1992) and Fodor (1995) most of the sub-basins of the Pannonian Basin are of transtensional origin. The Neogene Pannonian Basin itself is considered to be a flexural basin superimposed on a previous flexural Paleogene basin developed to the south of the inner Western Carpathian units (Tari *et al.*, 1993). According to Márton and Fodor (1995), rotation of smaller lithospheric blocks took place in the course of the extending of the inner Carpathian area.

The Neogene sediment formation of the Paratethys nearly took place simultaneously with the Cenozoic structural development of the Alpine-Carpathian orogenic system (Figure 1) (Brinkmann, 1966; Seneš, 1967). The basins on both sides of the uplifting ranges of the Carpathians comprise the so-called Central Paratethys. The flexural basins of the Central Paratethys in the inner Carpathians are called the Pannonian Basin, which is strongly disturbed by Miocene tectonic movements (Figure 2). Its Miocene sediment series have enough continuity for the sequence stratigraphic reconstruction; however, in the marginal sub-basins like the Nógrád, Borsod and Várpalota Basins, due to the intensive Miocene tectonic events, the magnitude of the unconformities is greater than average in the Pannonian Basin.

AGE AND ORIGIN OF THE SYNTECTONIC RHYOLITE TUFF ACCUMULATIONS IN THE MIOCENE

Age of the rhyolite tuff volcanism

The Miocene structural development of the Pannonian Basin was accompanied by a more-or-less continuous rhyolite tuff volcanism. The exploded materials of the most intensive periods of this volcanism are commonly referred to as 'horizons' of the rhyolite tuff complexes. The ages determined for these horizons are 19.6±1.4 Ma for the Gyulakeszi Rhyolite Tuff (GRF), 16.4±0.8 Ma for the Tar Dacite Tuff Formation (TDF), 13.7±0.8 Ma for the Sátoraljaújhely Rhyolite Tuff (SRF) and 12.5±0.5 Ma for the Szerencs Rhyolite Tuff (SZRF) (Hámor *et al.*, 1980; Gyalog, 2001).

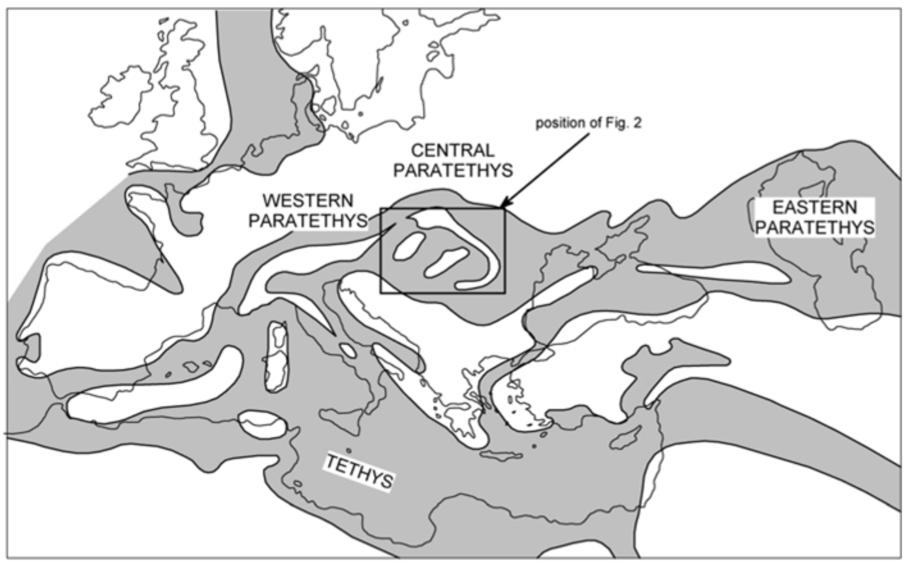

Figure 1. Position and paleogeographic sketch of the Paratethys during the Miocene (Seneš, 1967).

https://doi.org/10.1346/CCMN.2005.0530108 Published online by Cambridge University Press

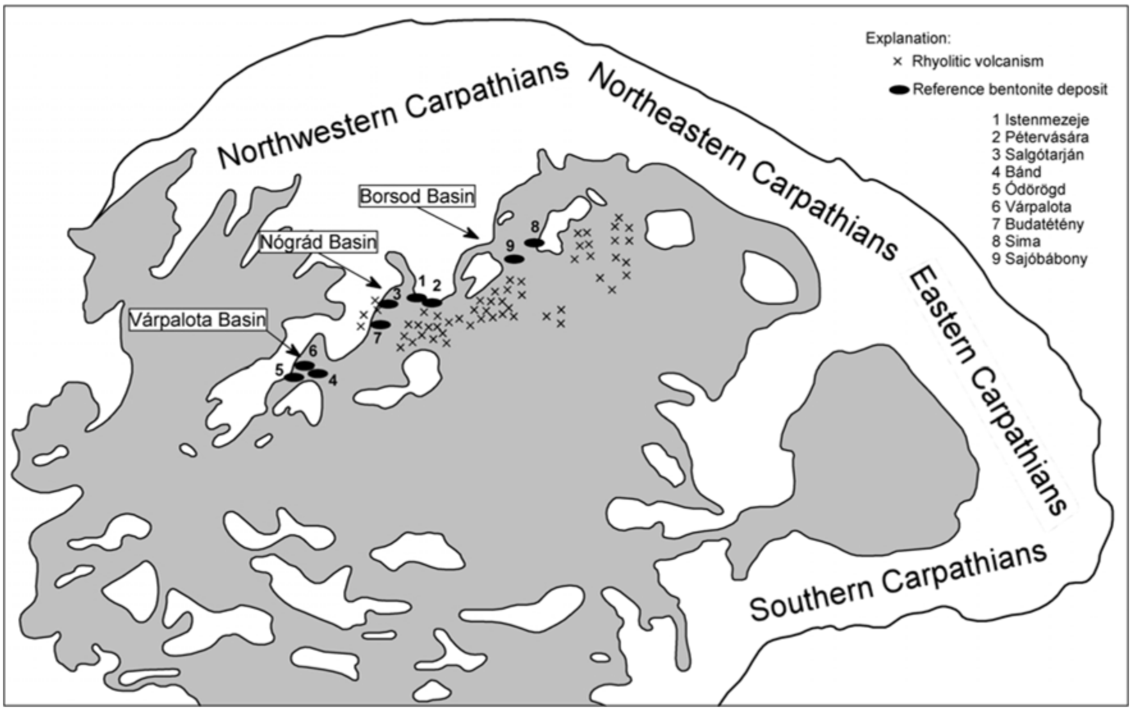

Figure 2. Paleogeographic map of the Pannonian Basin in the Miocene (Hámor, 2001).

However, the SRF and SZRF 'horizons' are, in fact, part of a continuous sequence of volcanogenic accumulation. To confirm the relatively continuous development of the tuff accumulation we collected, the previously published K/Ar radiometric data of rhyolite tuff samples taken from the northern part of Hungary within a region not wider than 150 km (Figure 3) were used. The data were measured at the Institute of Nuclear Research of the Hungarian Academy of Sciences (ATOMKI) in Debrecen and published in several papers over recent decades (*e.g.* Hámor *et al*., 1980; Széky-Fux *et al*., 1987; Márton and Pécskay, 1998).

The sampling areas (Figure 2) were the Tokaj Mountains, the foreland of the Bükk Mountains, the covered volcanics of the Great Hungarian Plain and some samples from the associated sub-basins of the Pannonian Basin like the Nógrád Basin. Data with uncertainty up to 1 m.y. were ignored and the maximum and minimum age of the samples are also demonstrated in the diagram. The radiometric data can also be found between the age intervals of the previously defined rhyolite tuff horizons and the accumulation can be regarded as continuous especially since 16.3 Ma.

Origin of the rhyolite tuffs

As demonstrated by petrological and geochemical investigations (Póka *et al*., 1998) the tuff complexes were derived from the melting of granite or metasedimentary formations of the upper crust. However, in the case of the TDF, the mixing of a rhyolitic and a mantle derived andesitic magma can be assumed.

The tectonically related uprising and eruption of the rhyolite tuffs are proven convincingly by paleomagnetic investigations (Szakács *et al*., 1998). The paleomagnetic data of the GRF indicate 80° counterclockwise rotation since the accumulation of the tuff complex, those of the TDF indicate 30° counterclockwise rotation, while in case of the SRF no rotation is indicated by the paleomagnetic records. The gradual decrease in paleomagnetic differences is interpreted as due to strong rotation of the basement accompanied by the rhyolite tuff volcanism.

Problem of the reworked tuffs

There is a long controversy on the appearance of reworked tuff horizons within the Miocene sediments. A sedimentological interpretation of the repeated occurrence of the tuff 'horizons' may be that they originated from the re-sedimentation of older tuff horizons. However, based on comparative mineralogical investigations there is evidence for repeated explosions (*e.g.* Kubovics *et al*., 1971). The radiometric data given in Figure 3 prove repeated volcanic eruptions.

EUSTASY AND SEDIMENTOLOGY OF THE PANNONIAN BASIN DURING THE MIOCENE

Vakarcs *et al*. (1998) reinterpreted the sedimentary formations of the Pannonian Basin from the aspect of sequence stratigraphy and correlated them with the sequences of the Central Paratethys and with those

https://doi.org/10.1346/CCMN.2005.0530108 Published online by Cambridge University Press

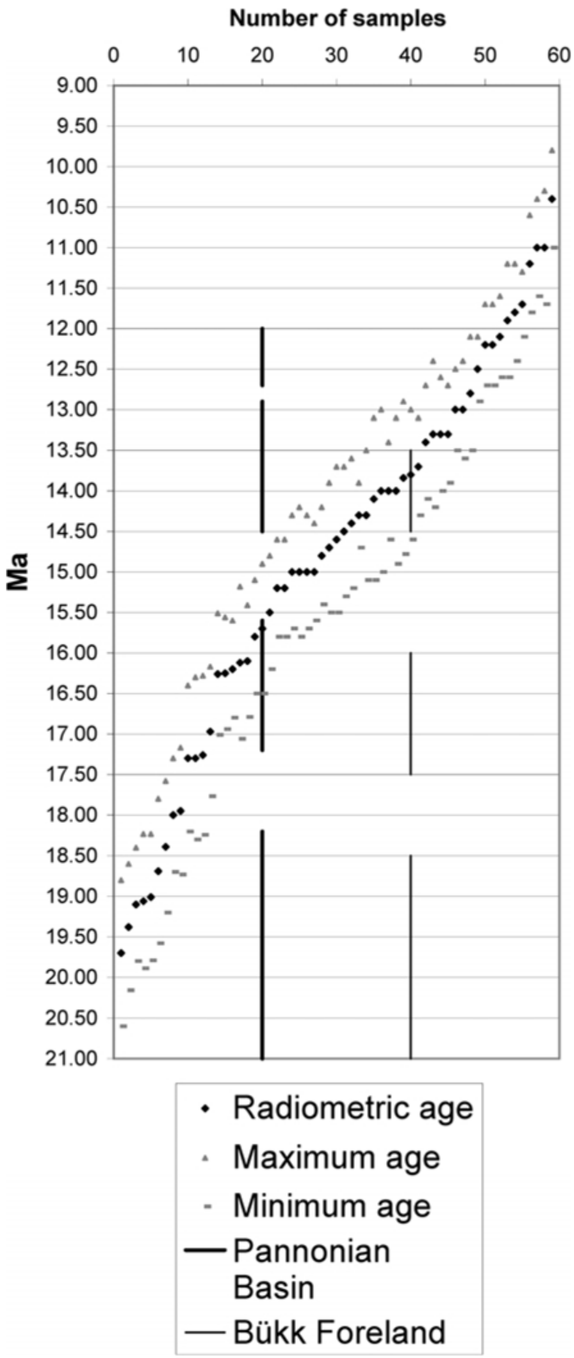

Figure 3. K/Ar radiometric data of the rhyolite tuffs in the Pannonian Basin and their relationship with the defined tuff horizons in the Pannonian Basin and in the Bükk Foreland.

defined by Haq *et al.* (1988). We applied their stratigraphic dissection (Figure 4) to the Central Paratethys correlating it with the Lithostratigraphic Units of the bentonite-bearing Borsod, Nógrád and Várpalota Basins demonstrated in Figure 2.

The Oligocene and Miocene sequences can barely be separated in the Pannonian Basin. The offshore conditions of the uppermost Oligocene and lowermost Miocene sequences are represented by the Szécsény Schlier Formation interfingering with the littoral, sub-littoral, occasionally brackish-lagoonal shoreline sandy facies of the Törökbálint Sandstone Formation (Báldi, 1997). The opening event of the Eggenburgian stage is the lower sequence boundary of the Bur-1 transgression. It is represented by the unconformity between the Szécsény Schlier Formation and the overlying Pétervására Sandstone Formation (Sztanó, 1994).

The Bur-2 transgression is represented by the occurrence of a transgressive surface within the Pétervására Sandstone Formation (Sztanó and Tari, 1993) in the NN2 nanoplankton zone (Nagymarosy, 1988). Terrestrial facies interfingering with the Pétervására Sandstone are represented by the Darnó Conglomerate while the overlying terrestrial series is the Zagyvapálfalva Variegated Clay Formation.

The Bur-3 transgression is represented at the base by the variegated fluvial and marsh sediments of the Nógrádmegyer Member and by formerly limnic, then paralic coal-bearing series of the Kisterenye Member of the Salgótarján Lignite Formation (Hámor, 1985). The latter is interfingered with the shallow marine silts of the Mátranovák Member. The sequence is closed by the regressive, burrowed, carbonaceous silty series of the Vizslás Sand Beds.

The Bur-4 transgression starts as a shoreline facies beginning with basal conglomerates represented by the Egyházasgerge Formation and continued by the thick offshore facies of the Garáb Schlier Formation within the NN4 nanoplankton zone (Horváth and Nagymarosy, 1979). The sequence is closed by the shallow-marine reef facies of the Fót Formation (Hámor, 1985).

The Lan-1 transgression is represented by variegated clay, silt and fine-grained sandstones of the Perbal Formation with tuff intercalations (Jámbor, 1997) and by the yellowish gray mollusc-bearing sandstone and lithothamnium mollusc-limestone of the Sámsonháza or Pécsszabolcs Formations which are frequently referred to as Leitha because of their former name 'Lower Leithkalk' (Hámor, 1997a). It has reef-archipelago facies and rich macrofauna. The sub-neritic facies is represented by the gray mollusc-bearing clay marl of the Baden Clay Formation rich in macro- and microfossils and accumulated in the NN5 nanoplankton zone (Nagymarosy, 1980). The upper part of the sequence is represented by the glauconitic sandstone and calcareous siltsone of the Pusztamiske Formation (Selmeczi, 1997).

The Lan-2/Ser-1 transgression is represented by a multiple seam lignite sequence and mollusc-bearing marl of the Hidas Lignite Formation (Kókay, 1966, 1967; Hámor, 1998) and by the Lithothamnium limestone of the Rákos Limestone Formation (Hámor, 1997b) beginning with conglomerate in some places. Offshore facies are represented by the foraminiferal clay marl of the Szilágy Clay Marl Formation (Hámor, 2001).

The Ser-2 transgression leads to the accumulation of the gray, greenish gray mollusc-bearing clay and clay marl series of the Kozárd Formation (Hámor, 1997c). At the brackish shoreline facies the mollusc-bearing calcareous sandstone of the Tinnye Formation were deposited. Fluvial and terrestrial sediments of this period are collected in the Sajóvölgy Formation (Hámor, 1985).

The existence and correlation of the Ser-3 transgression is indicated by the unconformity within the Kozárd Formation the age of which is well indicated by mollusc fauna referring to the Upper Sarmatian or in the Eastern Paratethys called Lower Bessarabian age of the upper part of the Kozárd Formation (Kókay, 1984; Püspöki *et al*., 2003). The fluvial-terrestrial and shoreline–nearshore facies of the sequence are represented by the various appearance of the Sajóvölgy Formation.

METHODS

To understand better the relationship between the bentonite formation and the eustatic and tectonic events we collected the stratigraphic, lithological, facies, mineralogical and geochemical data of the industrially most important Hungarian Miocene bentonite deposits and interpreted the data from the point of view of stratigraphic position and source material.

As the recently explored bentonite deposit at Sajóbábony may have significant industrial importance, 21 deep boreholes were planned, supported by a national research program (see the Acknowledgments section below) to evaluate the presence and the quality of the raw material. Fifteen of the deep boreholes were drilled taking core samples continuously. The total length of the drillings was 450 m, with >2000 samples taken. Only six of the boreholes produced geophysical data.

The facies characteristics of the deposit were described by macro- and microscopic investigation of 210 samples. Sedimentological analyses for grain-size distribution of 300 samples and micromineralogical analysis with the help of an optical microscope in 15 samples were made at the University of Debrecen.

X-ray diffraction measurements of 469 bentonitic samples from the core samples of the boreholes were carried out at the Geological Institute of Hungary to determine the mineralogy quantitatively. X-ray investigations were carried out by a PC-controlled Philips PW 1730 powder diffractometer with the following measurement conditions: Cu anticathode, 40 kV and 30 mA current, graphite monochromator, goniometer velocity 2°/min. Mineral quantity was determined from the relative rates of intensity of the characteristic reflections using either literature data or empirical corundum factors for each mineral (Klug and Alexander, 1954; Náray-Szabó *et al*., 1965; Rischák and Viczián, 1974; Rischák, 1989; Thorez, 1995).

The montmorillonite content was measured in two different ways for better determination based on 001 and 110 reflection intensities using different empirical factors, 0.7 and 1.5 respectively. This was necessary because most of the samples exhibited low-intensity diffuse 001 base reflections but sharp high-intensity 110 reflections. The averages of the different data were also calculated.

The thermal analyses were obtained by Derivatograph-PC with simultaneous TG, DTG and DTA set in a corundum crucible, with a heating speed of 10°C/min up to 1000°C and with Al_2O_3 as inert material. The quantitative determination of the thermally active minerals is based on the stoichiometric calculation of the heat-induced decomposition process of the identified minerals. The calculation measures mass deficit during the analysis. The thermal analyses were controlled by simultaneous measurements at the Department of Mineralogy and Geology of the University of Debrecen (Szöőr and Balázs, 2003).

Geochemical components as major elements from 35 samples and trace elements from 14 samples were investigated by inductively-coupled plasma-mass spectrometry (ICP-MS) at the Geological Institute of Hungary.

In order to detect the biostratigraphic position of the bentonite-bearing sedimentary series, we were able to prepare and document macrofossils from the core samples. The macrofauna was identified by I. Magyar (of MOL – the Hungarian Oil Company) and J. Kókay (of the Geological Institute of Hungary).

RESULTS

Bentonite deposits in the Miocene series of the North Hungarian Basin series

In Figure 4 we indicated the stratigraphic and facies position of the economically important sedimentary bentonite deposits of North Hungary. These deposits can be regarded as reference localities. Their main characteristics are listed below; some geological profiles can be seen in Figure 5 and their mineral and chemical contents are shown in Table 1.

Istenmezeje

The underlying series is pebbly glauconitic sandstone of the Pétervására Homokkõ Formation. The lower bed surface of the bentonite is the regional unconformity appearing within the Pétervására Sandstone and interpreted as a sequence boundary by Sztanó (1994). The lower layers of the bentonite deposit contain reworked intraclasts of the underlying series. The overlying series is the fine sandy facies of the Pétervására Sandstone Formation containing reworked clasts of the bentonite deposit (O. Sztanó, pers. comm.).

The lower part of the bentonite is intraclastic. It is overlain by a well-bedded yellowish bentonite, the base of which has lens-like bedding. The thickness of the beds is between 0.4 and 1.5 m. On the uppermost part of the

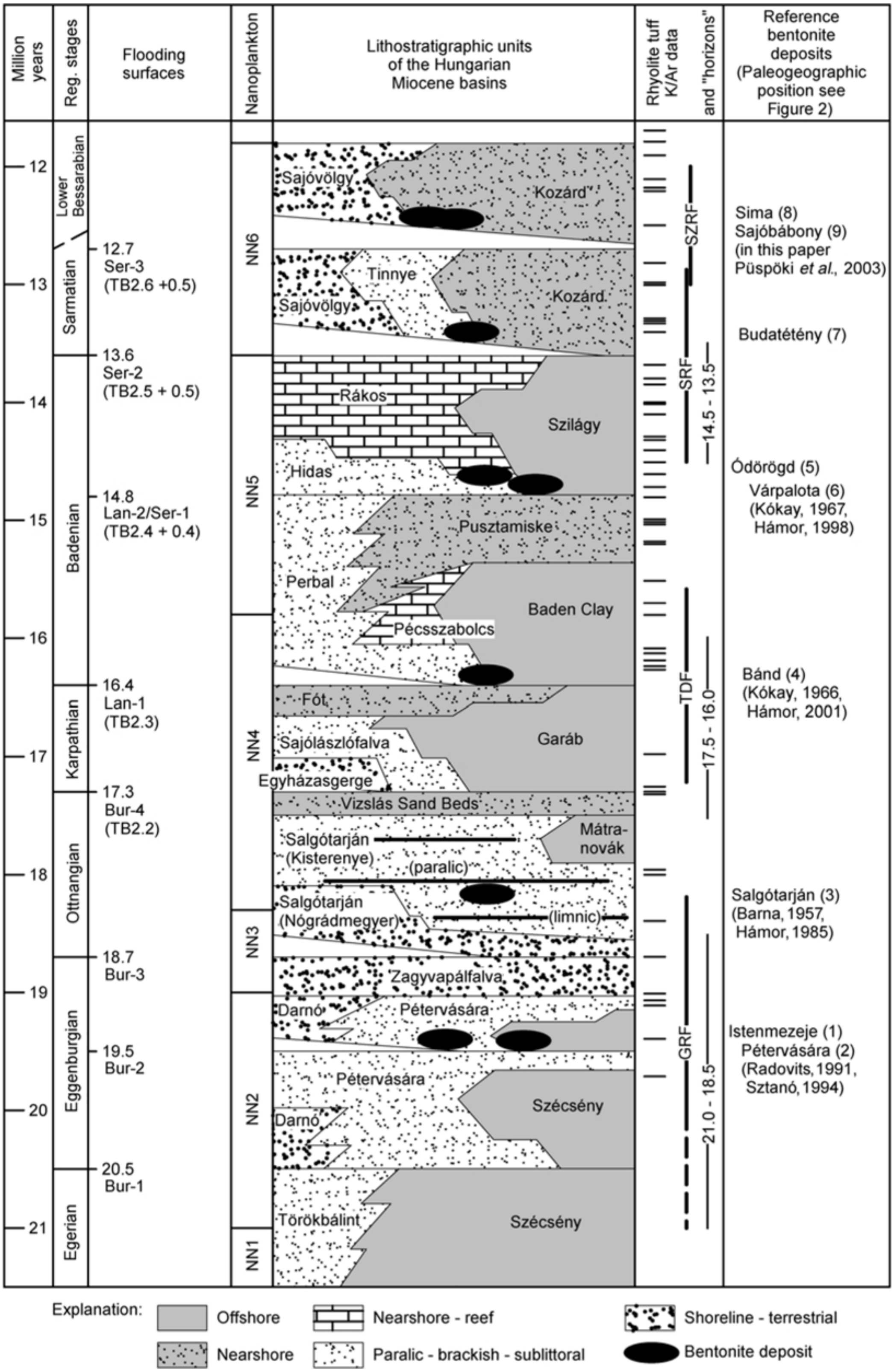

Figure 4. Stratigraphic position of the reference bentonite deposits and their relationship with the eustatic events and rhyolite tuff eruptions.

https://doi.org/10.1346/CCMN.2005.0530108 Published online by Cambridge University Press

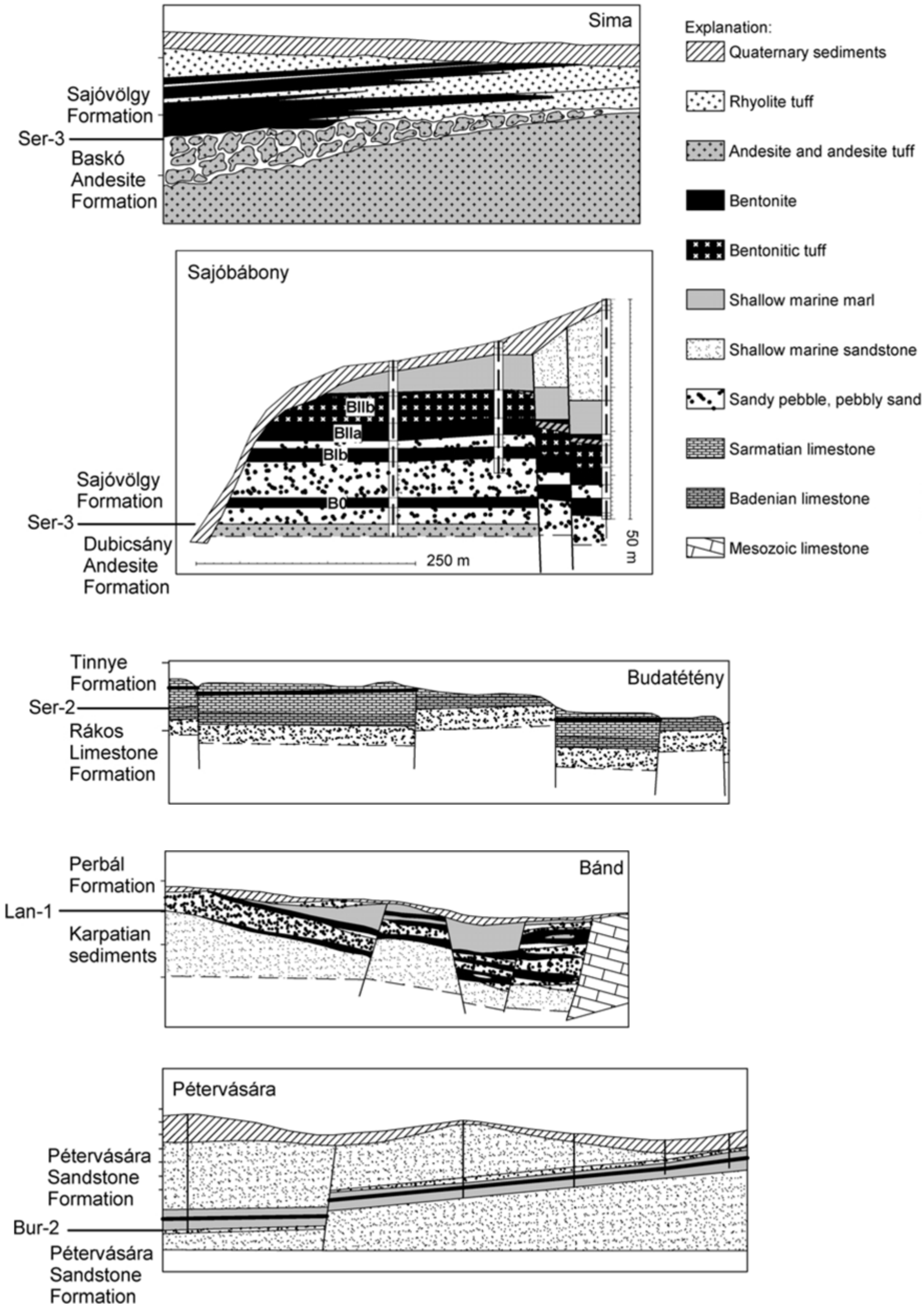

Figure 5. Sketch geological cross-sections of reference bentonite deposits.

https://doi.org/10.1346/CCMN.2005.0530108 Published online by Cambridge University Press

Table 1. Quantities (wt.%) of some mineral phases and major elements of bentonite samples from the reference bentonite deposits.

	Mineral phases				Major elements		
	Montmorillonite	Quartz	Cristobalite	Plagioclase	SiO_2	Al_2O_3	Fe_2O_3
Istenmezeje	50–80	1–25	10–40	1–5	60–65	13–17	2–4
Pétervására	50–60	3–5	32–35	3–5	68–69	15	2.6–2.8
Salgótarján	42–56	no data	no data	no data	69.2	16.6	2.28
Bánd	40–56	no data	no data	no data	55–57	17–26	2.5–3.5
Ódörögd	75	no data	no data	no data	no data	no data	no data
Budatétény	70–75		20–25		55–60	10–17	3–4

deposit, a gray sandy bentonite becomes dominant, showing similarity with the overlying sandy series (Radovits, 1991).

The source of the bentonite deposit is the GRF; the eustatic event is the Bur-2.

Pétervására

The age and stratigraphic position of the deposit are very similar to those of the Istenmezeje bentonite deposit (Sztanó, 1994). The under- and overlying series is the Pétervására Sandstone Formation; however, in the case of the Pétervására bentonite deposit the overlying series is a silty marl series of the Pétervására Sandstone Formation.

The depositional environments of the bentonite deposit were less disturbed than for the Istenmezeje bentonite, so the well-bedded yellowish bentonite type is dominant, with the sandy form subordinate (Radovits, 1991). The source of the bentonite deposit is the GRF; the eustatic event is the Bur-2.

Salgótarján

The underlying formation of the deposit is the variegated clay series of the Nógrádmegyer Member, its overlying series is the gray silt and silty clay or the second coal seam of the lignite-bearing series of the Salgótarján Lignite Formation (Hámor, 1985). The changing of the limnic character of the formation into paralic indicating the effect of the transgression can be correlated with the appearance of the bentonite deposit.

The material of the deposit is a white, yellowish white sometimes gray bentonite (Barna, 1957). The source of the bentonite deposit is the synchronously accumulated and reworked material of the GRF; the eustatic event is the Bur-3.

Bánd

The bentonite site lies unconformably on the eroded surface of the Karpatian series. The overlying materials are the mollusc-bearing clay-marls of the Baden Clay Formation. The formation can thus be correlated with the transgressive shoreline to nearshore series of the Perbál Formation (Hámor, 2001).

The series contains several bentonite layers interfingering with sandy coastal materials. The deposit contains three separate bentonite layers. The source of the bentonite deposit is the TDF; the eustatic event is the Lan-1.

Várpalota

The underlying formation is a basal conglomerate lying on the eroded surface of the Lower Badenian sequence. The overlying and partly enclosing series is the lagoonal Hidas Lignite Formation (Kókay, 1967; Hámor, 1998).

The deposit is composed of 7–8 bentonite layers with thicknesses ranging from 0.6 to 1.4 m and separated from each other by lignite seams on the top of the bentonite deposit. The material of the bentonite is not homogeneous; sandy and calcareous types can also be seen.

The source of the bentonite deposit is the rhyolite tuff erupted between the TDF and SRF or the oldest explosions of the SRF; the eustatic event is the Lan-2/Ser-1.

Ódörögd

The underlying series is the Triassic dolomite covered by a thin Miocene sandy clayey series. The covering series is the Lithothamnium limestone of the Rákos Formation.

The thickness of the bentonite layer varies between 0.8 and 2 m. It comprises a gray, greenish gray bentonite containing biotite; accessory minerals include kaolin and some carbonate minerals. The source of the bentonite deposit may be a rhyolite tuff eruption between TDF and SRF; the eustatic event is the Lan-2/Ser-1.

Budatétény

The underlying series of the bentonite deposit is Badenian yellowish and gray clay and sandy clay together with pebbly tuffaceous sandstone. The non-bentonitic intercalations and overlying strata of the deposit are composed of Sarmatian limestone of the Tinnye Formation.

The lower part of the Sarmatian series is a biogenic limestone with reef facies and with rich fossil association of coral and bryozoan species. The intercalations between the bentonite layers have a fragmented character occasionally with intraclasts and mollusc remnants.

The bentonite layers, ⩽0.5 m thick, are situated in the limestone series 2–3 and 15–20 m apart from each other. The bentonite can be dark green and rigid, sandy or yellowish gray with calcareous infiltrations. The source of the bentonite deposit might be the SRF; the eustatic event is the Ser-2.

Sajóbábony

The base of the series is a widely occurring andesite tuff horizon of the Dubicsány Andesite Formation; the overlying series is the mollusc-bearing greenish gray material of the Kozárd Formation (Püspöki *et al.*, 2003).

This deposit was explored recently so the stratigraphic interpretation and research is the most detailed. Based on the data of the deep drilling and natural outcrops the sequence begins with a terrestrial conglomerate at the bottom lying unconformably on the surface of the underlying andesite tuff horizon (Figure 6a). The overlying strata are well sorted and comprise well-bedded sandstone with cross stratification.

The first bentonite horizon (B0) has a thickness of 2–2.5 m. The montmorillonite content is 45–60%. This bentonite layer is covered by sandy facies of the shoreline called 'Lower placer' being 5–6 m thick. The increasing energy of the shallow marine shoreline unit is well demonstrated by reworked bentonitic clasts from the B0 horizon (Figure 6b) and by mostly oblique to vertical trace fossils and incomplete bioturbation by suspension feeding organisms (Figure 6c) (Bromley and Dávid, per. comm.).

The second bentonite horizon (BI) has a thickness of 1.8–2 m and its montmorillonite content is 45–60%. The bedding is laminar, though bioturbation can also be detected (Figure 6d). It is covered by not more than 2 m of thick sandy shoreline sediments. The sandy facies is similar to the 'Lower placer', the material may be arkose or placer in its character with the dominance of pyroxene due to the short transportation ('Upper placer'). Mainly immature cross-bedded sandstones, with small-scale ripple cross-lamination and frequently with exotic fragments, *e.g.* fine pumice intercalations or dust tuff fragments along the foreset beds can also be seen representing the sandy shoreline.

The third bentonite horizon (BIIa) has a thickness of >4 m. Its montmorillonite content is between 40 and 60%. The yellowish green material contains randomly distributed pumice fragments (Figure 6e).

The fourth bentonite horizon is represented by a series of strongly bentonitized rhyolite tuff beds ('bentonitic tuff' BIIb) with montmorillonite content from 30 to 60%. The rhyolite tuff was deposited under submarine conditions. In breaks in the tuff accumulation, the weathering of the formerly deposited tuff was continuous, initiating the formation of stratigraphically traceable changes in the quality of bentonitic tuff (Figure 6f). Overlying the 'bentonitic tuff', a bentonite horizon (BIII) <1 m thick appears, with a montmorillonite content of 60%.

Following the formation of the BIII bentonite horizon, open marine paleoconditions became dominant, with increasing silt and carbonate content. The thickness of the marine deposits reaches 10 m. In the lower part, well preserved index fossils are present (Figure 6g).

The overlying series is characterized by cyclic sedimentation of sandy silt and fine sandstone presumably representing a lower shoreface paleoenvironment with the dominance of sandy shorface facies gradually increasing upwards.

The source of the bentonite deposit might be the SZRF; the eustatic event is Ser-3.

Sima

Underlying the bentonite deposit is the fragmented and strongly weathered surface of a lower Sarmatian andesite complex (Baskó Andesite Formation). The overlying materials are pumiceous rhyolite tuff. The Upper Sarmatian age of the deposit can be determined from the microfossils of the neighboring limnic series deposited within a similar stratigraphic position. It has to be mentioned that several Hungarian geologists regard the series as liminic or limnic-paralic facies with brackish character so the relationship of the series with the flooding surface of the transgression is not entirely clear. However, the stratigraphic analogy with the well defined Sajóbábony deposit may refer to an analogy in the genetic aspect as well.

The bentonite is a greenish pelitic, subordinately sandy material. The mineralogy is dominated by montmorillonite (61–80%) with kaolinite (1–10%), cristobalite (11–26%) and opal (1–7%). K-feldspar can also be detected. Within the main elements, the SiO_2 content is 55.7%, Al_2O_3 is 15.9%, and Fe_2O_3 is 1.91% (Kovács-Pálffy, 1998).

The source of the bentonite deposit is thought to be the SZRF; the eustatic event is the Ser-3.

MINERALOGY AND CHEMISTRY OF THE SAJÓBÁBONY BENTONITE DEPOSIT

Based on the lithological characteristics of the bentonite horizons we could determine three main lithological types of bentonites in the whole bentonite-bearing series of Sajóbábony bentonite deposit:

(1) The bentonitic tuff is represented by samples from the BIIb layer. This lithological type has a primarily tuffaceous character, with bentonitic interbeddings and bentonitic clasts (Figure 6f). Along the small fractured zones of the reworked tuff small bentonitic veins can also be seen. The bentonitic layers and veins indicate the bentonitization of the tuff, but the tuffaceous matrix also has relatively high (20–30%) montmorillonite content.

(2) The tuffaceous bentonite is represented by a BIIa layer. This well-bedded greenish brown lithological type contains some reworked detrital minerals like muscovite and undulating quartz crystals and encloses numerous

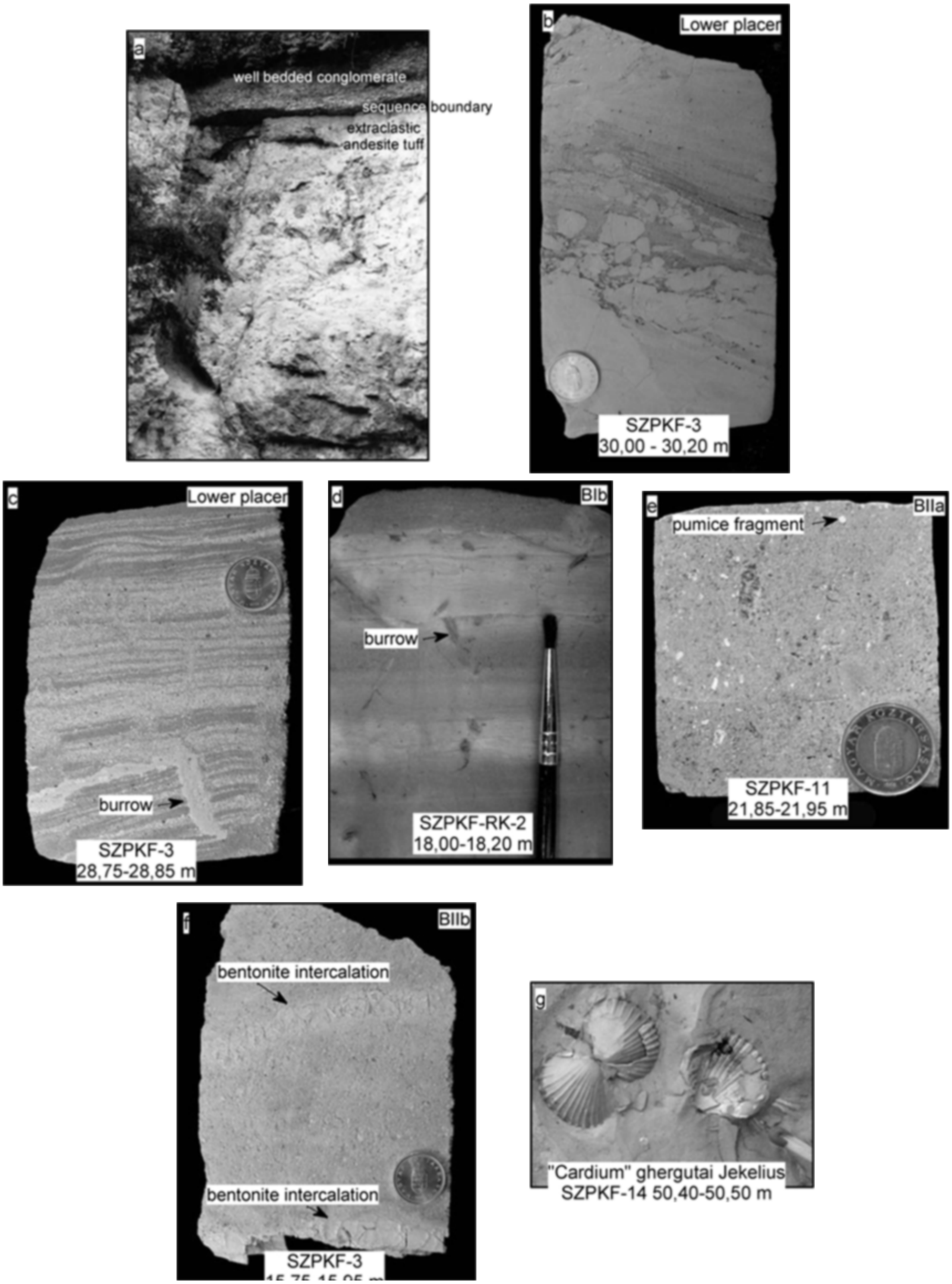

Figure 6. Characteristic facies of the Sajóbábony bentonite deposit. (a) Unconformity between the underlying andesite tuff horizon and the basal conglomerate of the bentonite-bearing series. (b) Reworked bentonite clasts at the boundary of the lowermost bentonite horizon (B0) and its overlying sandy faces ('Lower placer'). (c) Bioturbation in the sandy shoreline facies of the 'Lower placer'. (d) Laminated structure and bioturbation of the sedimentary bentonite (BIb). (e) Scattered pumice fragments in the texture of the tuffaceous bentonite (BIIa). (f) Bentonite intercalations in the bentonitic tuff (BIIb). (g) Lower Bessarabian index fossils in the overlying sandy marl.

https://doi.org/10.1346/CCMN.2005.0530108 Published online by Cambridge University Press

Table 2. Mean values of the mineral components of the different lithological types.

Facies type	*n*	Montmorillonite based on 001	Montmorillonite based on 110* reflection	Montmorillonite mean	Illite-mont.	Illite	Muscovite	Kaolinite-smectite	Kaolinite	Chlorite	Quartz	K-feldspar	Plagioclase	Calcite	Cristobalite	X-ray amorphous
Bentonitic tuff BIIb	133	31.56	35.92	33.74	3.95	5.74	0.30	0.03	0.14	0.89	7.94	6.93	13.11	0.23	6.05	22.56
Tuffaceous bentonite BIIa	120	33.04	33.98	33.51	4.06	5.89	1.17	0.17	0.34	1.63	14.03	5.40	17.45	0.27	3.28	13.08
Sedimentary bentonite BIb	175	44.37	38.29	41.33	3.66	4.43	3.65	0.01	0.14	0.99	10.45	4.06	16.48	1.71	1.27	8.32

* Multiplied by 1.5 (Ca-montmorillonite) empirical factor

small pumice fragments. The enclosed pumice fragments give the material a strong tuffaceous character (Figure 6e).

(3) The sedimentary bentonite is represented by B0, BI and BIII bentonite layers. This lithological type is a yellowish white material with generally >50% montmorillonite and no carbonate. Bedding is laminar, mainly graded, which may be due to the periodical submarine resedimentation or due to a periodical dust tuff accumulation with moderate intensity. Bioturbation can also be seen frequently on the bed surfaces (Figure 6d). These secondary deposits of smectite-rich clays are usually termed sedimentary bentonites (Grim and Güven, 1978).

The three lithological types represent variations in volcanic and sedimentary conditions. The first has dominantly tuffaceous character where the effect of the sedimentary processes is subdominant. The second has tuffaceous character with more apparent signs of sedimentary effects like the occurrence of detrital materials. The third lithological type has dominantly sedimentary character.

Considering the amount and size of the pumice fragments, the source material of the first and second lithological types was much coarser, however, still fine tuff, with crystals usually not larger than 0.1 mm whereas that of the third lithological type was a fine volcanic ash.

The mineralogical differences in the three lithological types of bentonites are well demonstrated by the stratigraphic distribution of the montmorillonite, and by geochemical investigations (Kovács-Pálffy, 1998). Thus the three main types were adequate for a detailed comparison between different bentonite types formed within the same transgressive systems tract.

X-ray powder diffraction analysis

Based on the investigation of 133 samples (Table 2), in the bentonitic tuff, clay minerals comprise the main mineral group (44%). Among the clay minerals, montmorillonite clearly dominates (77% of the clay) (Figure 7). Other clay minerals are illite-montmorillonite randomly mixed-layer minerals (9%) and illite ($2M_1$ >> $1Md$) (13%). The next dominant constituent is the amorphous phase (23%) with 7% K-feldspars and 13% plagioclase while the amount of quartz is no higher than 8% (Figure 8). Muscovite is present in six samples (4–9%).

Based on mean values from data of 120 samples in tuffaceous bentonite, the dominant fraction is also the clay mineral group, the content of which is similar to that of the bentonitic tuff (47%). Among clay minerals, montmorillonite is dominant – 72%). Other clay minerals are illite-montmorillonite randomly mixed-layer minerals (9%), illite ($2M_1$ >> $1Md$) (13%). Small amounts (1–5%) of kaolinite were also detected in 15 samples. The amount of the X-ray amorphous phase is

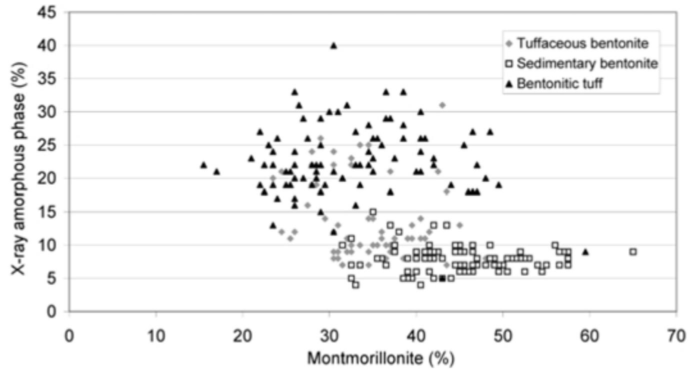

Figure 7. Distribution of the lithological types in the montmorillonite/amorphous phase diagram.

much less than that in the rhyolite tuff (13%). The quantities of feldspar are similar to those in the rhyolite tuff − 17% plagioclase, and 5% K-feldspar. The quartz content reaches 14%. Muscovite was detected in 19 samples (4−15%).

According to data from 175 samples, sedimentary bentonites have the greater quantities of clay minerals (54%) with montmorillonite dominant (76% within the clay mineral group). Other clay minerals are illite-montmorillonite randomly mixed-layer minerals (7%) and illite (8%). Kaolinite was detected only in 13 samples (1−4%). The amount of X-ray amorphous phase is the least significant (8%), the plagioclase content is 16% and that of K-feldspar is 4%. Quartz comprises 10% and muscovite was detected in 71 samples (4−16%).

Identification of the facies types on the XRD and DTG curves

The different facies of the bentonites are well represented by XRD patterns (Figure 9). In the case of the bentonitic rhyolite tuff, the 001 basal reflection of montmorillonite is weak and broad. The tuffaceous bentonite has a greater montmorillonite content and the sedimentary bentonite contains the most montmorillonite.

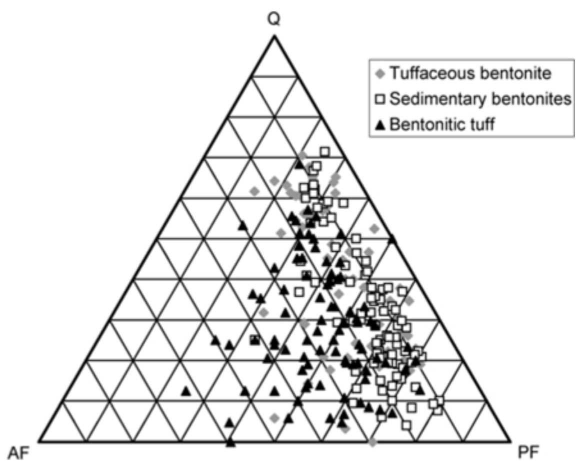

Figure 8. Distribution of the lithological types in the quartz/alkali feldspar/plagioclase system.

The existence of an X-ray amorphous phase is indicated by the thermal characteristics of the different bentonite types in Figure 10. The independent reaction of the X-ray amorphous phase can be seen as an important reaction between 240 and 280°C in the samples from the bentonitic tuff. This reaction is overlapped with those indicating that the molecular water content and the dehydroxylation of the clay mineral (indicated by hatched pattern in Figure 10) are superimposed on the dehydroxylation reaction of the X-ray amorphous phase spreading over a wide interval.

In the case of the tuffaceous bentonite, the existence of the X-ray amorphous phase is also characteristic. In the DTG curves it is easily observed since the dehydroxylation reaction of the montmorillonite does not return to the base line between 220 and 265°C but can extend even to 400°C as an elongated slope. For the sedimentary bentonite, the dehydroxylation of the montmorillonite is clearly separated into two steps. However, the fact that the curve does not return to the base line indicates the presence of some X-ray amorphous phase.

Geochemical data

Geochemical data were used primarily to demonstrate the degree of weathering in the various lithological types, secondarily to prove the common origin, and finally to indicate differences between the three different lithological types. Therefore, major elements, together with the X-ray amorphous phase indicate the degree of alteration. To investigate their genetic relationship, the trace element quantities of the bentonitic tuff and tuffaceous bentonite are compared.

Major elements were analyzed for 33 samples (Table 3) to investigate the geochemical changes initiated by weathering. The distribution of the samples in the Na_2O+K_2O–SiO_2 system (Le Bas *et al.*, 1986) reflects the strong decrease in alkaline elements and silica content due to bentonitization (Figure 11). The bentonitic tuff represents the least, the tuffogenic bentonite reflects the intermediate, and the sedimentary bentonite demonstrates the most intense degree of chemical weathering. On the ternary diagram of

https://doi.org/10.1346/CCMN.2005.0530108 Published online by Cambridge University Press

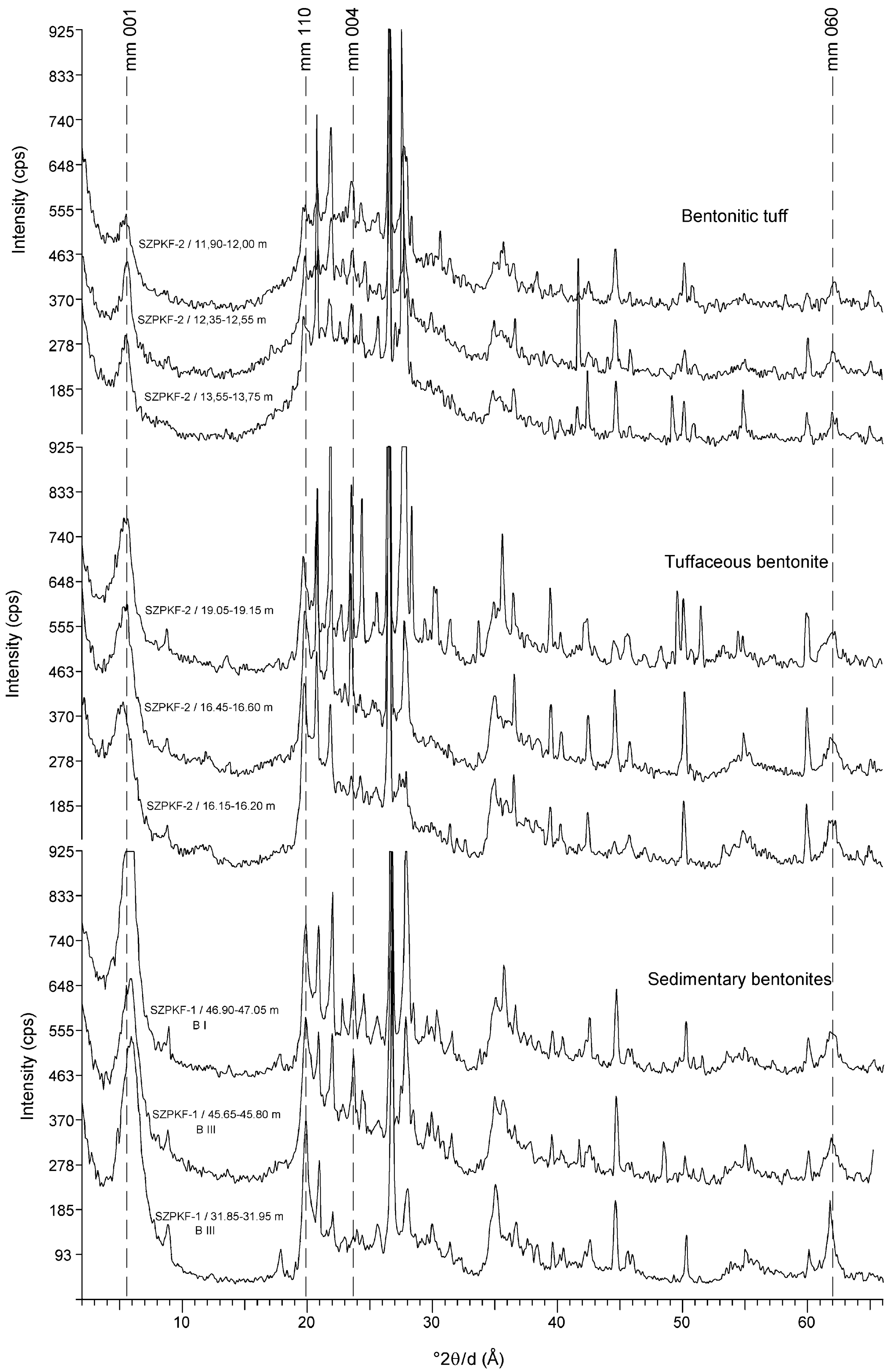

Figure 9. XRD patterns of the different lithological types.

https://doi.org/10.1346/CCMN.2005.0530108 Published online by Cambridge University Press

Table 3. Major-element compositions (wt.%) of bentonite samples from boreholes and outcrops.

	Borehole/ section	Depth	SiO_2	TiO_2	Al_2O_3	Fe_2O_3	FeO	MnO	CaO	MgO	Na_2O	K_2O	P_2O_5	SO_3	BaO	SrO	Loss on ignition	Total	Litholog-ical type
1	Kö valley	0.50–1.20	72.07	0.30	17.66	4.40		0.05	1.21	1.31	0.85	2.12	0.03					100.00	1
2	Kö valley	1.20–2.00	74.37	0.12	15.47	2.58		0.04	1.26	0.67	1.33	4.15	0.01					100.00	3
3	Kö valley	2.00–3.00	75.11	0.07	14.20	2.12		0.14	1.10	1.16	1.51	4.57	0.01					100.00	3
4	Kö valley	3.00–4.00	77.58	0.15	13.89	1.82		0.02	1.62	0.78	1.53	2.59	0.01					100.00	3
5	Kö valley	4.00–5.00	77.84	0.12	13.85	1.69		0.02	1.40	0.43	1.50	3.15	0.01					100.00	3
6	Kö valley	5.00–6.00	78.15	0.10	13.56	1.80		0.01	1.28	0.37	1.40	3.33	0.01					100.00	3
7	Kö valley	6.00–7.20	74.61	0.13	16.34	1.95		0.00	1.40	0.60	1.27	3.69	0.01					100.00	3
8	Kö valley	7.20–8.00	76.76	0.18	14.07	2.46		0.03	1.38	0.33	1.57	3.20	0.01					100.00	3
9	Kö valley	8.00–9.00	72.69	0.30	17.44	4.51		0.05	1.50	0.60	1.03	1.86	0.01					100.00	2
10	Kö valley	9.00–10.00	67.67	0.53	20.04	5.85		0.02	2.19	1.29	1.01	1.35	0.04					100.00	2
11	Kö valley	10.00–11.00	66.90	0.58	19.93	5.76		0.04	3.14	1.08	1.34	1.20	0.03					100.00	2
12	Kö valley	11.00–11.70	62.70	0.65	20.92	5.99		0.05	4.97	1.58	1.83	1.24	0.07					100.00	2
13	Kö valley	11.70–13.00	61.37	0.58	21.20	4.71		0.05	6.89	1.33	2.40	1.38	0.09					100.00	2
14	Kö valley	13.60–15.00	63.75	0.62	20.93	6.09		0.07	4.33	1.35	1.64	1.13	0.10					100.00	2
15	SZPKF-1	31.85–31.95	58.20	0.65	16.50	8.65	0.31	0.02	1.32	2.42	0.56	2.35	0.15	0.15	0.03	0.01	10.29	101.61	1
16	SZPKF-1	34.30–34.65	69.80	0.27	13.40	1.94	0.45	0.02	1.35	0.74	1.22	2.36	0.15	0.15	0.03	0.01	8.41	100.29	3
17	SZPKF-1	38.35–38.50	58.90	0.68	18.10	5.99	0.28	0.01	2.98	1.12	1.25	1.03	0.15	0.15	0.03	0.02	9.45	100.14	2
18	SZPKF-1	41.45–41.55	67.90	0.55	13.90	4.29	0.20	0.01	0.95	0.82	0.58	0.67	0.15	0.15	0.02	0.01	9.94	100.13	2
19	SZPKF-1	45.90–46.05	59.80	0.64	17.20	6.44	0.18	0.03	2.48	1.38	0.92	1.04	0.15	0.15	0.03	0.01	10.58	101.02	1
20	SZPKF-1	47.40–47.55	55.00	0.63	16.10	5.87	0.19	0.02	5.59	1.71	0.72	1.31	0.15	0.15	0.03	0.01	13.42	100.89	1
21	SZPKF-1	48.15–48.30	58.00	0.63	17.10	6.59	0.24	0.02	2.75	1.74	0.85	1.03	0.15	0.15	0.03	0.01	11.92	101.21	1
22	SZPKF-2	8.00–8.05	58.80	0.71	17.60	7.63	0.13	0.02	1.26	2.41	0.71	2.39	0.15	0.15	0.02	0.01	9.62	101.61	1
23	SZPKF-2	9.35–9.45	70.80	0.34	11.60	3.56	0.15	0.03	1.24	1.40	0.60	0.85	0.15	0.30	0.02	0.01	10.55	101.60	1
24	SZPKF-2	11.90–12.00	71.50	0.28	12.80	2.15	0.11	0.02	1.41	0.61	1.32	2.05	0.15	0.55	0.04	0.01	8.01	101.02	3
25	SZPKF-2	16.45–16.60	70.12	0.55	13.04	3.43	0.16	0.03	1.03	0.90	0.74	0.51	0.15	0.15	0.02	0.01	9.01	99.84	2
26	SZPKF-2	19.05–19.15	58.29	0.70	18.65	6.26	0.12	0.20	4.67	1.14	1.68	0.95	0.15	0.15	0.05	0.02	7.27	100.30	2
27	SZPKF-2	21.65–21.70	60.30	0.73	18.10	6.31	0.22	0.01	3.75	1.43	1.42	0.82	0.15	0.15	0.03	0.02	7.99	101.43	1
28	SZPKF-2	22.20–22.30	57.83	0.63	17.21	8.14	0.18	0.03	2.68	1.79	0.81	0.92	0.15	0.15	0.03	0.02	9.73	100.29	1
29	SZPKF-2	22.95–23.05	57.40	0.62	18.50	5.96	0.26	0.03	3.96	1.46	1.12	0.89	0.15	0.15	0.03	0.02	8.91	99.47	1
30	SZPKF-3	15.30–15.45	69.40	0.28	13.40	2.18	0.39	0.02	1.46	0.65	1.22	2.51	<0.15	<0.15	0.03	0.01	8.33	99.88	3
31	SZPKF-3	16.20–16.40	71.50	0.15	11.90	1.42	0.27	0.01	0.89	0.56	1.23	3.17	<0.15	<0.15	0.02	0.00	7.61	98.73	3
32	SZPKF-3	17.30–17.50	69.90	0.23	13.20	1.72	0.29	0.01	1.03	0.70	1.01	2.68	<0.15	<0.15	0.03	0.01	8.42	99.22	3
33	SZPKF-3	18.00–18.25	69.02	0.14	13.72	1.30	0.52	0.02	0.98	0.68	1.27	4.94	<0.15	<0.15	0.02	0.00	7.39	100.00	3

Analyzed by Mrs I. Török (Kö valley) 1998 and I. Barta (SZPKF) 1999; Lithological type: 1 – sedimentary bentonite, 2 – tuffaceous bentonite, 3 – bentonitic tuff

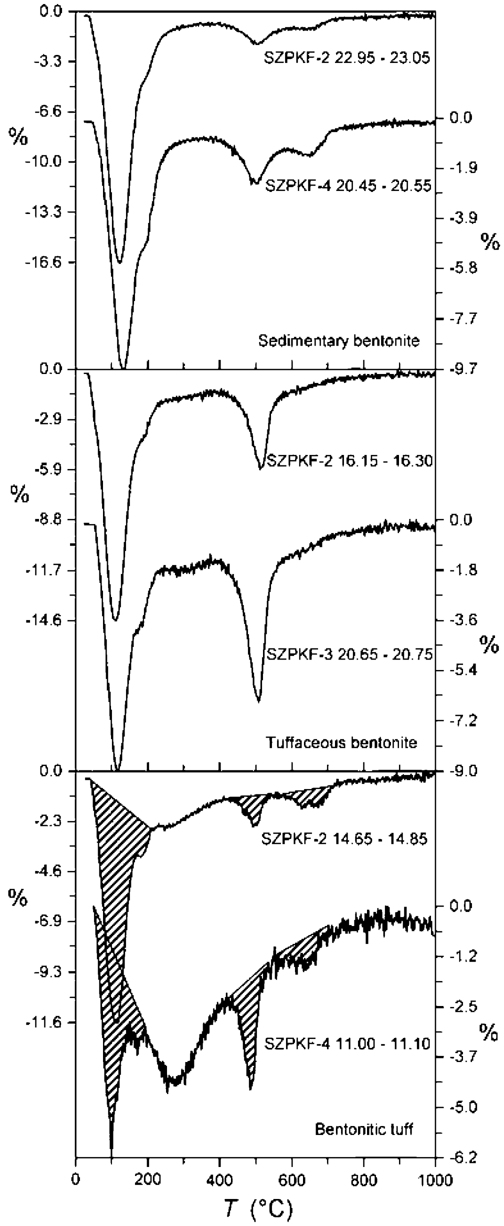

Figure 10. DTG and TG curves of the different lithological types.

Englund and Jörgensen (1973) (Figure 12) a decrease in alkaline elements occurs simultaneously with an increase in Fe and Mg during the weathering. The correlation between the amorphous phase and the silica content refers to the significant decrease of the X-ray amorphous phase with that of SiO_2 (Figure 13).

Trace element analyses of 14 samples (Table 4) were performed to evaluate the genetic connections between the bentonitic tuff and tuffaceous bentonite. Previous studies have shown that those elements which tend to be unaffected by weathering like Nb and Y are reliable indicators of the original character of parent rock (Teale and Spears, 1986; Merriman and Roberts, 1990; Rollinson, 1993; Huff *et al.*, 1997a, 1997b). Figure 14 shows the Nb/Y ratio of the samples which has an important role in demonstrating the genetic origin of igneous rocks (Winchester and Floyd, 1977) together with some elements like Cr, Co, V, Cu which could be transported into the sedimentary basin from the exhuming andesite tuff series, and with some elements like Sr, Ba reflecting submarine depositional conditions. The Nb/Y ratio is proved to be constant between the different facies types, whereas both the elements of andesite tuff origin and the elements reflecting submarine conditions separate the various facies conditions.

DISCUSSION

Stratigraphic interpretation of the reference bentonite deposits

Summarizing the data from the reference bentonite deposits described from the Pannonian Miocene series, some general characteristics can be stated. (1) All deposits have been deposited within marine or lagoonal series. (2) All were formed above regional discordances and their base is usually a kind of transgressive facies series like basal conglomerates. (3) The overlying series is composed of nearshore or open marine sediments of the subsequent sequence, so the bentonite-bearing series can be regarded as a transgressive series. (4) The appearance of the bentonite deposits is bedded and extensively distributed. (5) Considering the geochemical data, the source of the bentonites seems to be rhyolitic while the possibility of simultaneous volcanic eruptions cannot be excluded as the radiometric data regularly prove continuous rhyolite tuff volcanism. (6) In several cases the reworking of older tuffs and in some cases (Sima, Sajóbábony) the effect of underlying andesitic materials cannot be entirely excluded. (7) Comparing the stratigraphic position of the recently explored bentonite deposit at Sajóbábony, deductions can be made about its origin; moreover in the case of Sajóbábony – because of the significant amount of available data – further investigations could have been made to separate different facies types within the same transgressive systems tract.

MATERIALS OF THE SAJÓBÁBONY BENTONITE DEPOSIT

Source material

The tuffaceous character of the bentonite horizons is reflected by their mineral association. Most of the amorphous phase, the K-feldspar and plagioclase feldspar and some of the quartz may have originated from rhyolite tuff. The common source of the different lithological types is well represented by their distributions in the quartz/K-feldspar/plagioclase ternary diagram (Figure 8). In these figures a general overlap of the different facies types reflects the basically similar

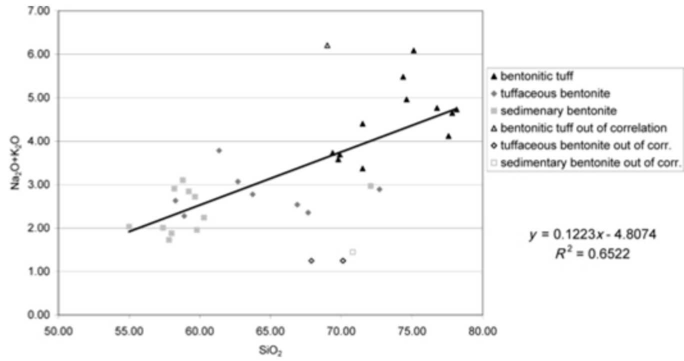

Figure 11. Position of the lithological types in the TAS diagram (Le Bas *et al.*, 1986).

quantities of the felsic minerals. Thus, quartz can also be regarded as being of volcanic origin as its amount is very similar in the different facies types.

The rhyolite tuff origin of the tuffaceous bentonite is also demonstrated by the existence of pumice fragments (Figure 6e). In the case of the sedimentary bentonite the tuffaceous origin can be proved by the ratio between quartz and feldspars. Notwithstanding the sedimentary character of the material, the amount of plagioclase is regularly three or five times as much as that of quartz also questioning a significant detrital quartz input. At the same time it must be noted that there may be significant geochemical and mineralogical contamination of the bentonite by reworked underlying andesite tuff. This is indicated especially by the higher Fe content (Figure 12), and confirmed by the fact that the under- and overlying sandy facies have placer character with the dominance of hypersthene which originated from the andesite tuff.

The general presence of illite-montmorillonite randomly ordered, mixed-layer phases (7–9%) also indicates the existence of reworked detrital minerals in the original rhyolite tuff layers.

The results from trace element analysis of the bentonitic tuff and tuffaceous bentonite (Figure 14)

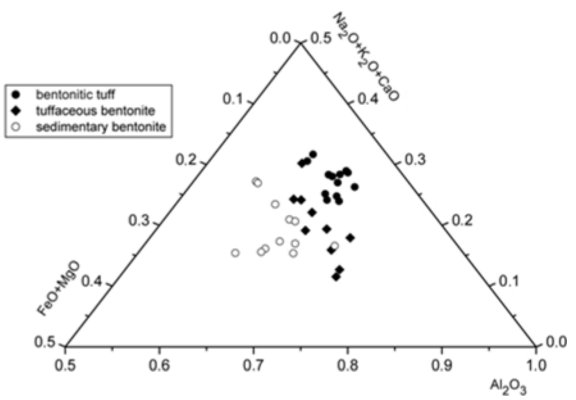

Figure 12. Distribution of the lithological types in the Na_2O+K_2O+CaO–Al_2O_3–FeO+MgO system (after Englund and Jörgensen, 1973).

indicate a constant Nb/Y ratio simultaneous with consequent increase of the concentration of the terrigenous elements from exhuming andesite tuffs (Cu, Cr, Co, V) and of some other elements reflecting the submarine depositional circumstances (Sr, Ba). The constant Nb/Y ratio also indicates a common source (the same rhyolite tuff series) for the bentonites while the consequent changes in the concentration of the other elements refer to the significant effect of the terrigenous contamination and the submarine paleoconditions.

Different degree of weathering

As mentioned above, the three lithological types can be regarded as three different cases from the point of view of the volcanic and sedimentological processes. These differences enabled the occurrence of three different levels of weathering and so of bentonitization.

These different levels of alteration are also very traceable by the connected interpretation of the XRD and DTA curves. The first indicate the differences in the intensity of the 001 reflections of the montmorillonite, while the latter is overprinted by the quantity of the amorphous phase. The main source of the bentonitic clays must have been the volcanic glass of the rhyolite tuff for which the degree of alteration should be well represented by the ratio between the amorphous phase and the montmorillonite (Figure 7). The bentonitic tuff at a less intensive degree of bentonitization has a higher volcanic glass content with the lower quantity of montmorillonite whereas, the tuffaceous bentonite at an intermediate level of alteration contains a much smaller quantity of volcanic glass and the more altered sedimentary bentonite contains a small amount of the X-ray amorphous phase and the greatest quantity of montmorillonite.

Major element data indicate a decreasing trend of Si, K and Na in the course of the bentonitization (Figure 11). From this aspect the assumed order in the degree of weathering is the same as that concluded from mineralogical data. The bentonitic tuff reflects a mainly tuffaceous character, the tuffaceous bentonite shows an intermediate level of alteration while the sedimentary

https://doi.org/10.1346/CCMN.2005.0530108 Published online by Cambridge University Press

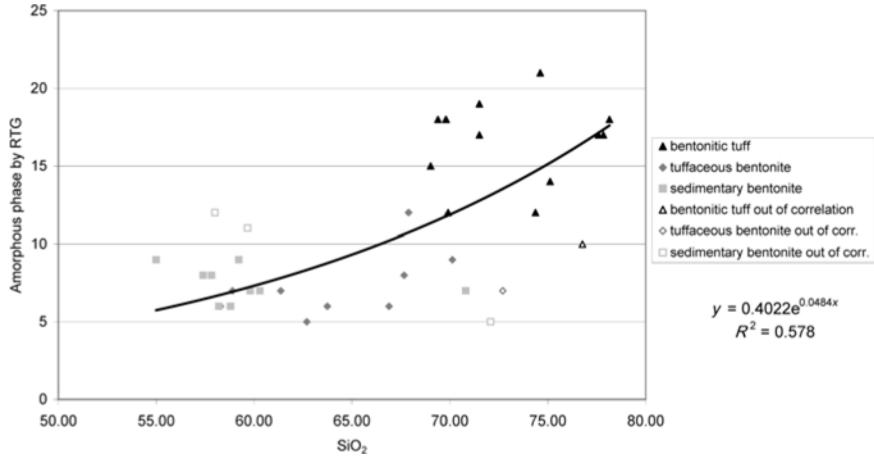

Figure 13. Correlation between SiO_2 content and the amount of the X-ray amorphous phase.

bentonite seems to be the most altered. The associated decrease of the SiO_2 content and the X-ray amorphous phase also indicates the volcanic source of the alteration.

Genetic model of the bentonite formation at Sajóbábony

Based on the facies development from the basal conglomerates through the shoreline paleoenvironments

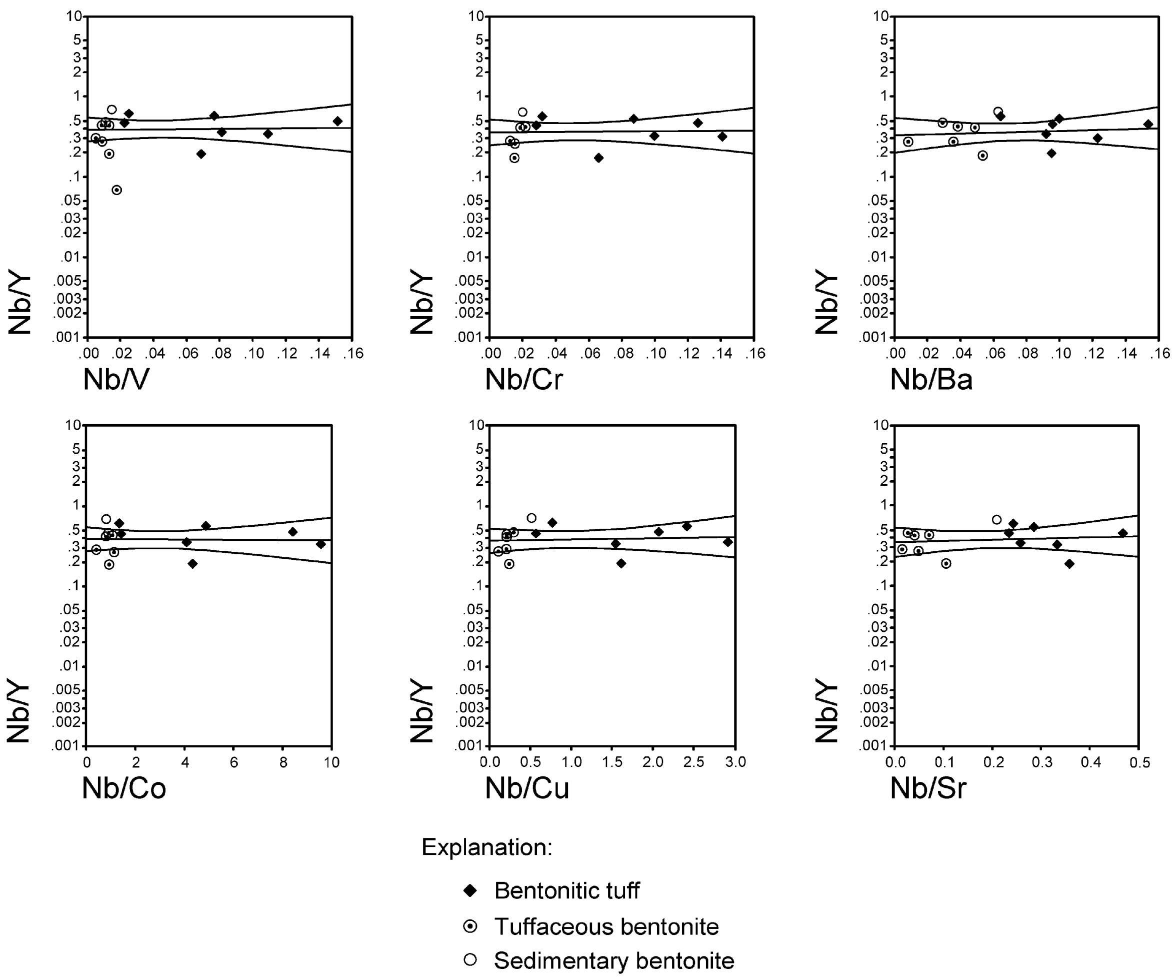

Figure 14. The trace element distributions of the different lithological types (Winchester and Floyd, 1977).

https://doi.org/10.1346/CCMN.2005.0530108 Published online by Cambridge University Press

Table 4. Trace element quantities of bentonites from the Kõ valley (mg/kg).

		Depth	Ba	Cd	Co	Cr	Cu	Ga	Ge	Li	Nb	Ni	Pb	Rb	S	Sr	V	Y	Zn	Lithological type
1	Kö valley	0.50–1.20	324	0.515	16.58	68.1	26.38	26.22	0.962	28.1	13.45	25.2	64.5	92.4	82	64.4	90	19.7	90.5	1
2	Kö valley	1.20–2.00	273	0.667	8.50	35.7	14.87	22.68	0.922	29.3	11.47	22.4	50.9	81.1	91	46.6	46	19.1	63.3	3
3	Kö valley	2.00–3.00	139	0.857	1.43	9.5	5.79	24.75	1.041	17.0	12.06	12.8	48.9	137.3	28	25.7	8	25.5	42.1	3
4	Kö valley	3.00–4.00	145	1.400	1.94	12.6	5.19	20.72	1.022	17.0	8.39	5.5	38.2	185.2	39	23.5	12	44.5	45.7	3
5	Kö valley	4.00–5.00	122	0.893	0.91	6.20	5.64	19.76	1.030	18.0	8.71	14.0	30.7	93.1	28	26.0	8	26.2	40.0	3
6	Kö valley	5.00–6.00	193	1.547	2.39	13.4	4.77	15.82	1.090	21.9	11.57	19.5	43.0	121.2	48	40.6	15	20.6	31.8	3
7	Kö valley	6.00–7.20	192	1.441	2.64	10.7	3.67	18.70	0.953	21.4	10.77	13.8	38.3	165.3	52	41.3	13	30.7	33.7	3
8	Kö valley	7.20–8.00	193	0.939	7.90	45.4	19.52	18.88	0.974	38.9	11.10	14.2	51.7	104.4	33	47.2	50	24.6	54.3	3
9	Kö valley	8.00–9.00	246	0.823	9.81	62.5	37.28	25.42	1.090	31.1	9.08	19.8	58.9	114.5	86	84.9	69	48.4	65.6	2
10	Kö valley	9.00–10.00	261	1.142	8.52	43.0	41.02	23.25	1.095	24.3	8.94	11.4	58.3	83.2	47	123.1	79	20.5	59.6	2
11	Kö valley	10.00–11.00	279	0.928	10.06	44.0	35.78	19.63	1.435	19.4	8.23	8.1	52.3	75.8	35	195.1	93	19.1	56.5	2
12	Kö valley	11.00–11.70	325	0.516	9.01	32.2	26.81	23.08	1.273	13.6	8.01	12.9	64.3	64.2	67	258.7	75	17.2	51.2	2
13	Kö valley	11.70–13.00	342	0.566	12.06	40.0	22.92	18.09	1.371	12.6	4.74	14.2	57.6	68.9	36	262.4	88	16.5	58.0	2
14	Kö valley	13.60–15.00	282	0.590	6.92	53.0	63.91	22.39	1.354	19.1	7.71	10.2	49.5	83.9	51	151.3	88	28.9	58.0	2

Analyzed by B. Kiss 1999; Lithological type: 1 – sedimentary bentonite, 2 – tuffaceous bentonite, 3 – bentonitic tuff

to the nearshore overlying strata, the series has transgressive character and considering the macrofauna data from the overlying sediments, it represents a transgressive systems tract (Ser-3). The sedimentary characteristics of the well-bedded, frequently laminated bentonite horizons embedded into the usually cross-laminated, frequently burrowed sandy series reflect the deepening water conditions related to the flooding surfaces of the transgressive system tract.

Based on the mineralogical and geochemical data, the main source of the bentonite deposits was rhyolite tuff which, according to the radiometric data of the rhyolite volcanism in the Pannonian Basin, could have originated from a synsedimentary tuff accumulation controlled by a synchronous tectonic activity of the region. The contamination effect of reworked material of the underlying andesitic tuff horizon cannot be excluded, but the similarity of the mineral quantities, the ratio between quartz and feldspar minerals and the data from trace element analyses refer to similar synsediment tuff accumulations.

The differences between the lithological types of the bentonite were caused by the different degrees of weathering of the X-ray amorphous phase. Presumably the weathering has been determined by the tuff accumulation rate and the simultaneous sedimentation rate, in which case the three lithological types of the explored bentonite deposit may represent different relationships between the sedimentation and tuff accumulation rates as follows:

(1) Low sedimentation rate due to the intensive transgression simultaneous with a limited tuff accumulation rate and with accumulation of extremely fine dust tuffs of high specific surface area (B0, BI) accompanied by sedimentary reworking could lead to the formation of 'sedimentary bentonite'.

(2) Low sedimentation rate because of the intensive transgression, however, with the occasional occurrence of detrital input, synchronous with a more intensive accumulation of coarser rhyolite tuff with pumices led to the formation of the 'tuffaceous bentonite' (BIIa).

(3) The low sedimentation rate due to the continuous transgression connecting with a much more intensive, although periodical, tuff accumulation could form 'bentonitic tuff' (BIIb). During breaks in the tuff accumulation, the formation of thin bentonite intercalations took place (Figure 6f).

CONCLUSIONS

Seven economically important 'reference bentonite deposits' were investigated in the Miocene basin-filling sediment series of the Pannonian Basin. Considering their material characteristics and stratigraphic position the following conclusions can be made:

(1) Each investigated bentonite deposit is related to a transgressive series of a given sedimentary sequence.

(2) Considering the available radiometric data, each transgressive series containing a bentonite deposit can be correlated with an important, continuous rhyolite tuff explosion period of the Pannonian Miocene.

(3) Permanent rhyolite tuff explosion simultaneous with a highstand systems tract can initiate bentonite formation but presumably because of the significant terrigenous siliciclastic contamination and because of the fast infill of the sedimentary basin, the formation of significant bentonite deposits is rare.

(4) Transgressive series without intensive and continuous tuff accumulation (*e.g.* Bur-3), because of the lack of source material, cannot lead to the formation of significant bentonite deposits, although small bentonite interbeddings related to short, episodic explosions may also be detected.

(5) Consequently, the role of the synergism of the tuff accumulation and eustatic events can be assumed where the source material of the bentonites is the rhyolite tuff, while the paleoecological condition of the weathering is the transgression development causing condensed sedimentation, providing enough time for the optimal alteration of the volcanic material.

(6) To clarify the role and importance of the reworked older rhyolite tuffs as possible source material for the 'reference bentonite deposits', further investigations are required, especially on the structure of the montmorillonite and the quantities of the accessory mineral assemblages. Some arguments related to this question were investigated in the bentonite deposit at Sajóbábony.

Three lithologically and technologically different bentonite horizons of the bentonite deposit at Sajóbábony – representing three different bentonitic facies types within the same transgressive series – were investigated from two aspects. The first was to clarify the source material, the second was to determine the causes of the differences. From the data from X-ray, thermal and geochemical investigations the following conclusions can be drawn.

(1) Considering the similar character of the felsic minerals (quartz, K-feldspar, plagioclase), a common rhyolitic source for the bentonite facies is suggested. For the bentonitic tuff and tuffaceous bentonite, the constant Nb/Y ratio also proves the common rhyolitic source.

(2) In the case of the lowermost horizon – sedimentary bentonite – the existence of the reworked material from the underlying andesite tuff series is presumed. This contamination of terrestrial origin becomes less significant for the intermediate horizon, presumably because of the gradual covering of the surrounding terrains by the material of the transgressive series.

(3) The main difference between the facies types is the degree of weathering. The bentonitic tuff is the least altered, the tuffaceous bentonite represents an intermediate degree of alteration and the sedimentary bentonite is the most weathered material. Considering the ratio between the X-ray amorphous phase and the montmorillonite and the well correlated associated decrease of the X-ray amorphous phase and the SiO_2 content, the amorphous volcanic glass can be regarded as the main source of the montmorillonite formation. The different levels of the alteration can also be seen in the TAS diagram proving the strong decrease of the alkaline elements in the course of the bentonitization.

Our opinion is that the possibility, and the level, of weathering within a transgression series are determined by the changing of the tuff accumulation and the sedimentation rate as follows. The transgression decreases the sedimentation rate below a critical level allowing the optimal alteration of the X-ray amorphous phase of the rhyolite tuff depositing in submarine conditions. Therefore the bentonite horizons represent the time intervals with the lowermost sedimentation rate. With increasing accumulation rate of the terrigenous siliciclastic sediment, bentonite formation stops because of the strong mixing of the authigenic and detrital minerals. At the same time the increasing intensity of the tuff accumulation itself can limit the bentonite formation because rapid deposition and covering prevent optimal alteration of the X-ray amorphous phase. This is well represented by the lower degree of bentonitization in the case of the bentonitic tuff.

Summarizing the results from the stratigraphic interpretation of the 'reference bentonite deposits' and comparative analyses of the different bentonite horizons regarded as lithological types within the same transgressive systems tract from Hungary, we can state that the relationship of the tectonic-related tuff accumulation and eustasy-related sedimentation rate can be regarded as an important factor that determines the possible formation of bentonite in the long term and the degree of the bentonitization in the short term.

ACKNOWLEDGMENTS

The exploration of the Sajóbábony bentonite deposit was supported by the National Research and Development Fund (3/083/2001), the stratigraphic investigation by the Fund of Research and Development in the Higher Education (049/2000), and by the National Scientific Research Found (T029058). The authors thank I. Magyar (Hungarian Oil Company) and J. Kókay (Geological Institute of Hungary) for identifying the Sarmatian molluscs, and R. Bromley (University of Copenhagen) and Á. Dávid (Karoly Eszterhazy College, Eger) for determining the trace fossils. We are also thankful to colleagues in the Hungarian Geological Institute for helping with material examinations and especially to Associate Editor Professor Warren D. Huff (University of Cincinnati) for his encouragement in preparing this publication and useful comments on the English, the structure and the content of the paper.

REFERENCES

Báldi, T. (1997) *Lower Miocene Lithostratigraphy of North Hungary* (János Haas, editor). In commemoration of József

https://doi.org/10.1346/CCMN.2005.0530108 Published online by Cambridge University Press

Fülöp, pp. 215–230 (in Hungarian). Academic Press, Budapest.

Balla, Z. (1986) Analysis of the anti-clockwise rotation of the Mecsek Mountains (Southwest Hungary) in the Cretaceous: Interpretation of palaeomagnetic data in the light of the geology. *Geophysical Transactions ELGI*, **32,** 147–181.

Barna, J. (1957) Investigation of Na-bentonite bearing rhyolite tuff from Salgótarján. *Bányászati Lapok*, **1**, 10–14 (in Hungarian).

Brinkmann, R. (1966) *Abriss der Geologie II. Historische Geologie*. Ferdinand Enke Verlag, Stuttgart, Germany, pp. 1–343.

Englund, J.O. and Jörgensen, P. (1973) A chemical classification system for argillaceous sediments and factors affecting their composition. *Geologiska Föreningens i Stokholm Förhandlinger*, **95**, 87–97.

Fodor, L. (1995) From transpression to transtension: Oligocene-Miocene structural evolution of the Vienna basin and the East Alpine-Western Carpathian junction. *Tectonophysics*, **242**, 151–182.

Grim, R.E. and Güven, N. (1978) *Bentonites – Geology, Mineralogy and Uses*. Developments in Sedimentology, **24**, Elsevier, Amsterdam, 256 pp.

Gyalog, L. editor (2001) Proposals for the Hungarian Stratigraphic Committee to introduce (or modify) new stratigraphic units in the joint project of the Hungarian Geological Institute and the MOL Ltd. in the Tokaj Mts – Nyírség, the North Hungarian Mountain Range, the mouth of the Sió river and the Transdanubian Mts regions based on the deep drilling interpretations and the constructions of 1:100000 maps between 1998–2000. Hungarian Geological Institute, pp. 1–40 (in Hungarian).

Hámor, G. (1985) Geology of the Nógrád-Cserhát area. *Geologica Hungarica Series Geologica*, **22**, 1–307.

Hámor, G. (1997a) Sámsonháza Formation. P. 41 in: *Basic Lithostratigraphic Units of Hungary – Charts and short descriptions* (G. Császár, editor). The Geological Institute of Hungary, Budapest.

Hámor, G. (1997b) Rákos Limestone Formation. P. 40 in: *Basic Lithostratigraphic Units of Hungary – Charts and short descriptions* (G. Császár, editor). The Geological Institute of Hungary, Budapest.

Hámor, G. (1997c) Kozárd Formation. P. 39 in: *Basic Lithostratigraphic Units of Hungary – Charts and short descriptions* (G. Császár, editor). The Geological Institute of Hungary, Budapest.

Hámor, G. (1998) *Miocene Stratigraphy of Hungary in Geological Formations of Hungary*. Special publication of Hungarian Oil Ltd. and the Geological Institute of Hungary, pp. 437–454 (in Hungarian).

Hámor, G. (2001) *Miocene palaeogeography of the Carpathian Basin – Explanatory notes to the Miocene palaeogeographic maps of the Carpathian Basin 1:3,000,000*. The Geological Institute of Hungary, Budapest, p. 70.

Hámor, G., Ravasz-Baranyai, I., Balogh, Kad. and Árva-Soós, E. (1980) Radiometric age of Hungarian Miocene rhyolite tuff horizons. *Annual Report of the Hungarian Geological Institute for 1978*, pp. 65–74 (in Hungarian).

Haq, B.U., Hardenbol, J. and Vail, P.R. (1988) *Mesozoic and Cenozoic chronostratigraphy and Cycles of Sea-level change – Sea-Level Changes. An Integrated Approach*. SEPM Special Publication **42**, Society of Sedimentary Geology, Tulsa, Oklahoma, USA.

Horváth, F. (1993) Towards a mechanical model for the formation of the Pannonian Basin. *Tectonophysics*, **225**, 333–358.

Horváth, M. and Nagymarosy, A. (1979) The age of the Rzehakia Beds and the Garáb Schlier Formation based on nannoplankton and foraminifera research. *Bulletin of the Hungarian Geological Society*, **109**, 211–229 (in Hungarian).

Horváth, F. and Royden, L. (1981) Mechanism for the formation of the Intra-Carpathian Basins: a review. *Earth Evolution Science*, **3**, 307–316.

Huff, W.D., Bergström, S.M., Kolata, D.R. and Sun, H. (1997a) The Lower Silurian Osmundsberg K-bentonite. Part II: mineralogy, geochemistry, chemostratigraphy and tectonomagmatic significance. *Geological Magazine,* **135**, 15–26.

Huff, W.D., Morgan, D.J. and Rundle, C.C. (1997b) *Silurian K-bentonites of the Welsh Borderlands: Geochemistry, mineralogy and K-Ar ages of illitization*. British Geological Survey, Report WG/96/45, 25 pp.

Jámbor, Á. (1997) Perbal Formation. P. 41 in: *Basic Lithostratigraphic Units of Hungary – Charts and short descriptions* (G. Császár, editor). The Geological Institute of Hungary, Budapest.

Klug, H.P. and Alexander, L.E. (1954) *X-ray Diffraction Procedures*. John Wiley & Sons Inc., New York-London-Paris, 716 pp.

Kókay, J. (1966) Geological and paleontological analysis of the lignite deposit at Herend and Márkó. (A herend márkói barnakõszénterület földtani és õslénytani vizsgálata) *Geologica Hungarica ser. Paleontologica*, **36**, 1–149 (in Hungarian).

Kókay, J. (1967) Upper Tortonian Formations of the Bakony Mountains (A Bakony-hegység felsõtortónai képzõdményei). *Bulletin of the Hungarian Geological Society*, **97**, 74–90 (in Hungarian).

Kókay, J. (1984) New data relating to Moldavian structural events. *Annual Report of the Hungarian Geological Institute for 1982*, 501–503 (in Hungarian).

Kovács-Pálffy, P. (1998) Comparative mineralogical, geochemical and genetic investigations of Tertiary bentonite type mineral deposits. PhD thesis, Eötvös Lóránd University of Sciences, Budapest (in Hungarian).

Kovács, S. (1982) Problems of the "Pannonian Median Massif' and the plate tectonic concept. Contributions based on the distribution of Late Paleozoic – Early Mesozoic isopic zones. *Geologische Rundschau*, **71**, 617–639.

Kozák, M., Püspöki, Z. and McIntosh, R. (2001) Structural development outline of the Bükk Mountains reflecting recent regional studies. *Acta Geographica Debrecina*, **35**, 135–174.

Kubovics, I., Pécsiné, Dónáth É., Rózsavölgyi, J., Nagyné Balogh, J. and Andó, J. (1971) *Complex petrological, geochemical and volcanological investigation of sedimentary and volcanic formations from the Cserhát Mts. – Complex REE research in the Cserhát, Final Report*. Unpublished manuscript, Eötvös University, Department of Petrology and Geochemistry, Budapest, 710 pp. (in Hungarian).

Le Bas, M.J., Le Maitre, R.W., Streckeisen, A. and Zanettin, B. (1986) A chemical classification of volcanic rocks based on the Total Alkali-Silica diagram. *Journal of Petrology*, **27**, 745–750.

Márton, E. and Fodor, L. (1995) Combination of palaeomagnetic and stress data – a case study from North Hungary. *Tectonophysics*, **242**, 99–114.

Márton, E. and Pécskay, Z (1998) Complex evaluation of paleomanetic and K/Ar isotope data of the Miocene ignimbritic volcanics in the Bükk Foreland, Hungary. *Acta Geologica Hungarica*, **41**, 467–476.

Merriman, R.J. and Roberts, B. (1990) Metabentonites in the Moffat Shale Group, Southern Uplands of Scotland: Geochemical evidence of ensialic marginal basin volcanism. *Geological Magazine*, **127**, 259–71.

Nagymarosy, A. (1980) Correlation of the Badenian in

Hungary. *Bulletin of the Hungarian Geological Society*, **110**, 206–245 (in Hungarian).

Nagymarosy, A. (1988) *Nannoplankton stratigraphic investigations on the core samples from deep drillings near the seismic cross sections across the North Hungarian Paleogene Basins*. The Geological Institute of Hungary, Budapest, 50 pp.

Náray-Szabó, I., Zsoldos, L. and Kálmán, A. (1965) *Introduction to XRD Structure Investigation*. Association of Hungarian Chemists, Budapest, 305 pp. (in Hungarian).

Póka, T., Szakács, A., Seghedi, I., Simonits, A., Zelenka, T. and Nagy, G. (1998) Petrology and geochemistry of the Miocene acidic explosive volcanism of the Bükk Foreland, Pannonian Basin, Hungary. *Acta Geologica Hungarica*, **41/4**, 437–466.

Püspöki, Z., Kozák, M., Csámer, Á., McIntosh, R. and Vincze, L. (2003) Paleogeographic conditions and sequence stratigraphy of the Sarmatian sediment series in the Tardona Hills. *Bulletin of the Hungarian Geological Society*, **133**, 191–210 (in Hungarian).

Radovits, L. (1991) *Report on bentonite exploration around Istenmezeje-Váraszó-Erdõkövesd-Pétervására in 1991*. The Geological Institute of Hungary, Budapest.

Rischák, G. (1989) Direct XRD determination of amorphous phase in rocks and soils. *Annual Report of the Geological Institute of Hungary from 1987*, 377–394 (in Hungarian).

Rischák, G. and Viczián, I. (1974) Factors infuencing the base reflection intensity of clay minerals. *Annual Report of the Geological Institute of Hungary from 1972*, 229–256 (in Hungarian).

Rollinson, H. (1993) *Using Geochemical Data: Evaluation, Presentation, Interpretation*. Longman, London, 352 pp.

Schmidt, T., Blau, J. and Kázmér, M. (1991) Large-scale strike-slip displacement of the Drauzug and the Transdanubian Mountains in early Alpine history: Evidence from permo-mesozoic facies belts. *Tectonophysics*, **200**, 213–232.

Selmeczi, I. (1997) Pusztamiske Formation. P. 41 in: *Basic Lithostratigraphic Units of Hungary – Charts and short descriptions* (G. Császár, editor). The Geological Institute of Hungary, Budapest.

Seneš, J. (1967) Chronostratigraphie und Neostratotypen. Miozän M_3, Miozän der Zentralen Paratethys. *Vydavatelstvo Slovenskej akademie vied*, Bratislava, 1–312.

Szakács, A., Márton, E., Póka, T., Zelenka, T., Pécskay, Z. and Seghedi, I. (1998) Miocene acidic explosive volcanism in the Bükk Foreland, Hungary: Identifying eruptive sequences and searching for source locations. *Acta Geologica Hungarica*, **41**, 413–435.

Széky-Fux, V., Pécskay, Z. and Baloh, Kad. (1987) Covered volcanites and their K/Ar radiometric chronology from the Northern and Middle Transtibiscian region. *Bulletin of the Hungarian Geological Society*, **117**, 223–235 (in Hungarian).

Szöőr, Gy. and Balázs, É. (2003) *Thermal Analysis of Core Samples from SzPKF Deep Drillings*. Published by the University of Debrecen, Hungary, 120 pp. (in Hungarian).

Sztanó, O. (1994) The tide-influenced Pétervására Sandstone, Early Miocene, Northern Hungary: Sedimentology, Palaeogeography and basin development. PhD thesis, University of Utrecht, The Netherlands, 155 pp.

Sztanó, O. and Tari, G. (1993) Early Miocene basin evolution in Northern Hungary. *Tectonophysics*, **226**, 485–502.

Tari, G., Horváth, F. and Rumpler, J. (1992) Styles of extension in the Pannonian Basin. *Tectonophysics*, **208**, 203–219.

Tari, G., Báldi, T. and Báldi-Beke, M. (1993) Paleogene retroarc flexural basin beneath the Neogene Pannonian Basin: A geodynamic model. *Tectonophysics*, **226**, 433–455.

Teale, C.T. and Spears, D.A. (1986) The mineralogy and origin of some Silurian bentonites, Welsh Borderland, UK. *Sedimentology*, **33**, 757–765.

Thorez, J. (1995) *Practical Clay Geology*. Eötvös Lóránd University, Short Course note **2**. Budapest, pp. 15–25.

Vakarcs, G., Hardenbol, J., Abreu, V.S., Vail, P.R., Várnai, P. and Tari, G. (1998) *Oligocene – Middle Miocene Depositional Sequences of the Central Paratethys and their Correlation with Regional Stages*. SEPM Special Publication **60**, pp. 209–231. Society for Sedimentary Geologisists, Tulsa, Oklahoma, USA.

Winchester, J.A. and Floyd, P.A. (1977) Geochemical discrimination of different magma series and their differentiation products using immobile elements. *Chemical Geology*, **20**, 325–343.

(*Received 1 December 2003; revised 9 September 2004; Ms. 862; A.E. Warren D. Huff*)